Electronic Supplementary Information

Dielectric relaxation of deep eutectic solvent + water mixtures: Structural implications and application to microwave heating

Vira Agieienko*[a] and Richard Buchner[b]

[a]Department of Physical Chemistry, A. M. Butlerov Chemical Institute, Kazan (Volga Region) Federal University, 420008 Kazan, Russian Federation. E-mail: vera.n.ageenko@gmail.com

[b]Institute of Physical and Theoretical Chemistry, University of Regensburg, 93040 Regensburg, Germany. E-mail: richard.buchner@chemie.uni-regensburg.de

S1 Materials and methods

DES/water mixtures were prepared by adding degassed Millipore Milli Q water to Schott bottles containing an appropriate amount of DES prior weighed in a glovebox. In contrast to many previous studies, we used a pseudo-component molar mass definition for DESs written as $M^*_{\mathrm{DES}} = M_{\mathrm{ChCl}} + 2 \times M_{\mathrm{HBD}}$ which yields 323.81 and 259.74 g·mol^{-1} for glyceline and reline, respectively. Accordingly, the nominal DES mole fraction in DES/water mixtures was defined as

$$x_1 = \frac{m_1/M^*_1}{m_1/M^*_1 + m_2/M_2} \tag{S1}$$

where M_2 is molar mass of water, the m_i are the masses of DES ($i = 1$) and water ($i = 2$). The thus defined DES mole fraction relates to the mole fractions of the individual DES components as $x_{\mathrm{ChCl}} = x_1/(2x_1 + 1)$ and $x_{\mathrm{urea}} = 2x_1/(2x_1 + 1)$ and DES equivalent molarity as

$$c_1 = c_{\mathrm{ChCl}} = \frac{x_1\rho}{M_1x_1 + M_2(1 - x_1)}. \tag{S2}$$

The latter quantity was required for the quantitative evaluation of dielectric relaxation amplitudes. In addition, both quantities, x_1 and c_1, calculated from M^*_1 allow the direct comparison of properties of DES/molecular liquid (ML) mixtures for DES with different salt-to-HBD compositions, as well as with properties of conventional electrolytes, ionic liquids (IL) and IL/ML mixtures at equivalent composition.

Density, $\rho(x_1)$, necessary for calculating DES molarity, c_1, eqn (S2), and analytical water concentration, $c_2 = c_{\mathrm{w}}$, in DES/water mixtures was obtained at $T = 298.15$ K using an Anton Paar DMA 5000M vibrating-tube type densimeter operating within a temperature stability of 0.005 K and with a measurement repeatablity of $\pm 5 \times 10^{-3}$ kg·m^{-3}.

Dynamic viscosity, $\eta(x_1)$, was estimated from $\rho(x_1)$ and kinematic viscosities determined with an Anton Paar AVM rolling-ball viscometer at $T = 298.15$ K. Depending on the mixture viscosity, glass capillaries with an inner diameter of 1.6, 1.8, 3.0 and 4.0 mm were used. Capillaries were calibrated with viscosity standards S3, N14, N44, and N415 purchased from Canon Instrument Company.

Electrical conductivity, $\kappa(x_1)$, was obtained using a LCR Bridge (Hameg HM 8118) connected to home-built two-electrode capillary cells. Temperature control was performed with a calibrated Pt100 sensor connected to an ASL F250 precision thermometer and adjusted by a Huber Unistat 505 thermostat within ± 0.005 K. To eliminate electrode polarization, the resistance, R, was recorded as a function of frequency, ν, between 100 Hz and 10 KHz and its limiting value, $R_\infty = \lim_{\nu\to\infty} R(\nu)$, was extracted using the empirical function $R(\nu) = R_\infty + A/\nu^a$ with the A parameter specific to the cell and $a \approx 0.5$.

The data for ρ, η, κ of the studied glyceline/water mixtures, as well as calculated c_1 values, are listed in Table S1 as a function of the nominal DES mole fractions, x_1, calculated from the used masses of DES (m_1) and water (m_2) with eqn (S1). Table S1 also gives corrected DES mole fractions, x_1^{corr}, accounting for the residual water content of the used glyceline. Since the relative difference between x_1 and x_1^{corr} is smaller than the uncertainty of the dielectric data, the nominal DES mole fraction was used throughout in their evaluation. For reline/water the corresponding data at $T = 298.15$ K were taken –or interpolated if necessary– from ref. [1].

Table S1: Molarity, c_1, density, ρ, dynamic viscosity, η, electrical conductivity, κ at $T = 298.15$ K for glyceline/water mixtures as a function of nominal DES mole fraction, x_1. Also included are values x_1^{corr} accounting for the residual water content of the DES.

x_1	x_1^{corr}	c_1/mol·dm^{-3}	ρ/kg ·m^{-3}	η/mPa·s	κ/mS·cm^{-1}
0.000	0.000	0.000	997.05	0.898	–
0.010	0.010	0.486	1025.41	1.238	32.26
0.025	0.025	1.029	1057.11	1.910	44.46
0.050	0.050	1.638	1091.57	3.540	40.58
0.075	0.075	2.038	1113.51	5.965	31.94
0.100	0.100	2.321	1128.50	9.533	21.15
0.150	0.150	2.693	1147.44	18.68	13.13
0.200	0.199	2.925	1158.72	31.19	12.11
0.250	0.249	3.084	1166.23	46.32	6.976
0.300	0.299	3.201	1171.48	64.31	5.332
0.400	0.399	3.358	1178.32	106.6	3.453
0.499	0.497	3.458	1182.61	151.0	2.536
0.599	0.597	3.528	1185.55	197.1	1.974
0.699	0.695	3.580	1187.61	242.1	1.629
0.800	0.795	3.620	1189.18	286.8	1.416
0.897	0.891	3.651	1190.43	330.9	1.246
1.000	0.992	3.678	1191.44	370.3	1.109

Dielectric relaxation spectroscopy. Dielectric properties of the DES/water mixtures were recorded in the frequency range $0.05 \leq \nu/\mathrm{GHz} \leq 89$ at $T = (298.15 \pm 0.05)$ K. For 0.05 to 50 GHz two open-ended coaxial-line probe kits, Agilent 85070E-020 and Agilent 85070E-050, connected to a vector network analyzer (VNA, Agilent E8364B) were used to obtain relative permittivity, $\varepsilon'(\nu)$, and total loss, $\eta''(\nu)$ from the recorded reflection coefficient. A two-step calibration procedure was applied to correct for imperfections of the network-analyzer system [2] and errors arising from the difference in the dielectric properties of the sample and the load calibrant. As primary calibration standards air (empty cell), purified mercury (short) and as the load standard water (glyceline/water) or propylene carbonate (reline/water) were used. For the second step three liquids (including the load calibrant from the primary calibration) with known dielectric properties were measured together with the samples to obtain frequency-dependent correction parameters with a complex Padé approximation [3]. The selected secondary standards depended on the DES and on mixture composition. For glyceline/water butanol and dimethylacetamide were used for all mixture compositions. For reline/water mixtures at $x_1 \leq 0.2$ water and dimethylacetamide were used. At higher reline content dimethylacetamide and n-butanol were chosen.

To cross-check the reflection measurements, additionally data covering $26.4 - 40.0$ GHz were measured for selected glyceline/water mixtures and all reline/water mixtures using a variable-pathlength waveguide transmission cell hooked to the VNA as this setup does not require calibration. Also no calibration was required for the waveguide interferometer covering $60 \leq \nu/\mathrm{GHz} \leq 89$ [4].

The thus obtained spectra (symbols) are shown in Figure S1.

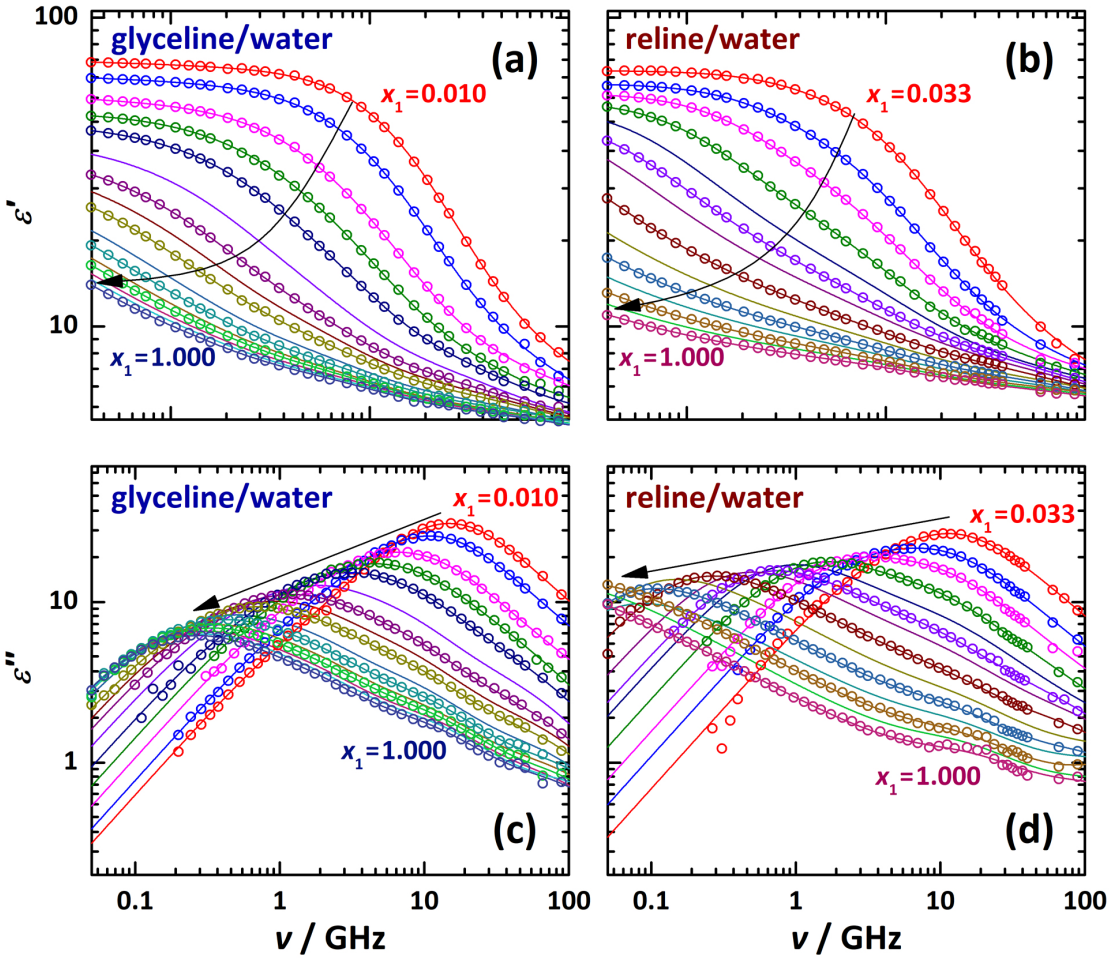

Figure S1: Spectra of relative permittitivy, ε' (a, b), and dielectric loss, $\varepsilon'' = \eta'' - \kappa/(2\pi\nu\varepsilon_0)$ (c, d), of glyceline/water (a, c) and reline/water (b, d) mixtures at $T = 298.15$ K covering the entire miscibility range, $0.0 < x_1 \leq 1.0$. Symbols represent the experimental data, lines the fits with the 5D (a, c) or the CD+2D (b, d) model. The arrows indicate the direction of increasing DES concentration. For clarity only every second experimental point is shown.

S2 Choice of the best fitting model

The choice of the best fitting model for DES/water mixtures was based on a few general criteria [5]:

- The chosen model should preferably provide the best fit, ie. have the smallest value of the reduced error function

$$\chi^2_{\mathrm{r}} = \frac{1}{2N-m-1}\left[\sum_{i=1}^{N} w_{\varepsilon'}(\nu_i)\delta\varepsilon'(\nu_i)^2 + \sum_{i=1}^{N} w_{\varepsilon''}(\nu_i)\delta\varepsilon''(\nu_i)^2\right] \tag{S3}$$

  In this equation $\delta\varepsilon'(\nu_i) = \varepsilon'(\nu_i) - \varepsilon'_{\mathrm{fit}}(\nu_i)$ and $\delta\varepsilon''(\nu_i) = \varepsilon''(\nu_i) - \varepsilon''_{\mathrm{fit}}(\nu_i)$ are the residuals of the simultaneously fitted relative permittivity, $\varepsilon'(\nu)$, and dielectric loss, $\varepsilon'(\nu)$, data with weights $w_{\varepsilon'}$ and $w_{\varepsilon''}$; N is the number of data triples $(\nu_i, \varepsilon'(\nu_i), \varepsilon''(\nu_i))$, and m the number of the adjustable parameters. Since χ^2_{r} is normalized it allows comparing models with different m [6].

- Fit parameters should have physically reasonable values and vary smoothly with composition.

- The number of resolved modes should reasonably comply to the mixture composition.

  Expected are contributions arising from the dipolar DES components, either as a single relaxation or a sum of modes, and water. However, cross-correlations among the dipolar species might be possible and modes may overlap due to comparable relaxation times.

- The fit parameters obtained for the mixtures should recover the limiting values defined by the neat compounds.

  Since the dielectric spectrum of neat water in the microwave region is a superposition of two Debye relaxations centered at ∼18 GHz ($\tau_{\mathrm{coop}} = 8.35$ ps, $S_{\mathrm{coop}} = 72.418$) and ∼570 GHz ($\tau_{\mathrm{f}} = 0.278$ ps, $S_{\mathrm{f}} = 2.43$) at 298.15 K [7, 8], both modes should be detected at least for water-rich mixtures (although the fast mode might be problematic as its amplitude is small and it peaks outside the covered frequency range of 0.05 to 89 GHz). Vice versa, for DES-rich mixtures the modes resolved for the neat deep eutectic solvents (and/or its individual dipolar components) should be found.

Keeping in mind these criteria, the experimental dielectric spectra were evaluated by simultaneously fitting $\varepsilon'(\nu)$ and $\varepsilon''(\nu)$ to relaxation models based on sums of $n = 1 \ldots 5$ Havriliak-Negami (HN) equations or their simplified variants [9]. In all fits weights were kept to unity. The outcome of this procedure can be summarized as follows.

Glyceline/water mixtures. The left panel of Fig. S2 compares relative deviations, $\delta_{\mathrm{r}} = \delta\varepsilon''/\varepsilon''$, of the experimental dielectric loss data, $\varepsilon''(\nu)$, from their fit values, $\varepsilon''_{\mathrm{fit}}(\nu)$, obtained with the HN, CC+2D, 4D and 5D models at glyceline mole fractions $x_1 = 0.100, 0.500$ and 1.000. As expected from the shape of the spectra (Fig. S1a & c), a single HN relaxation (collapsing to CC for $x_1 < 0.100$) can reasonably fit $\varepsilon''(\nu)$ (and $\varepsilon'(\nu)$) over the entire mixing range and the obtained parameters look reasonable (Fig. S3a-d). However, with increasing glyceline content,

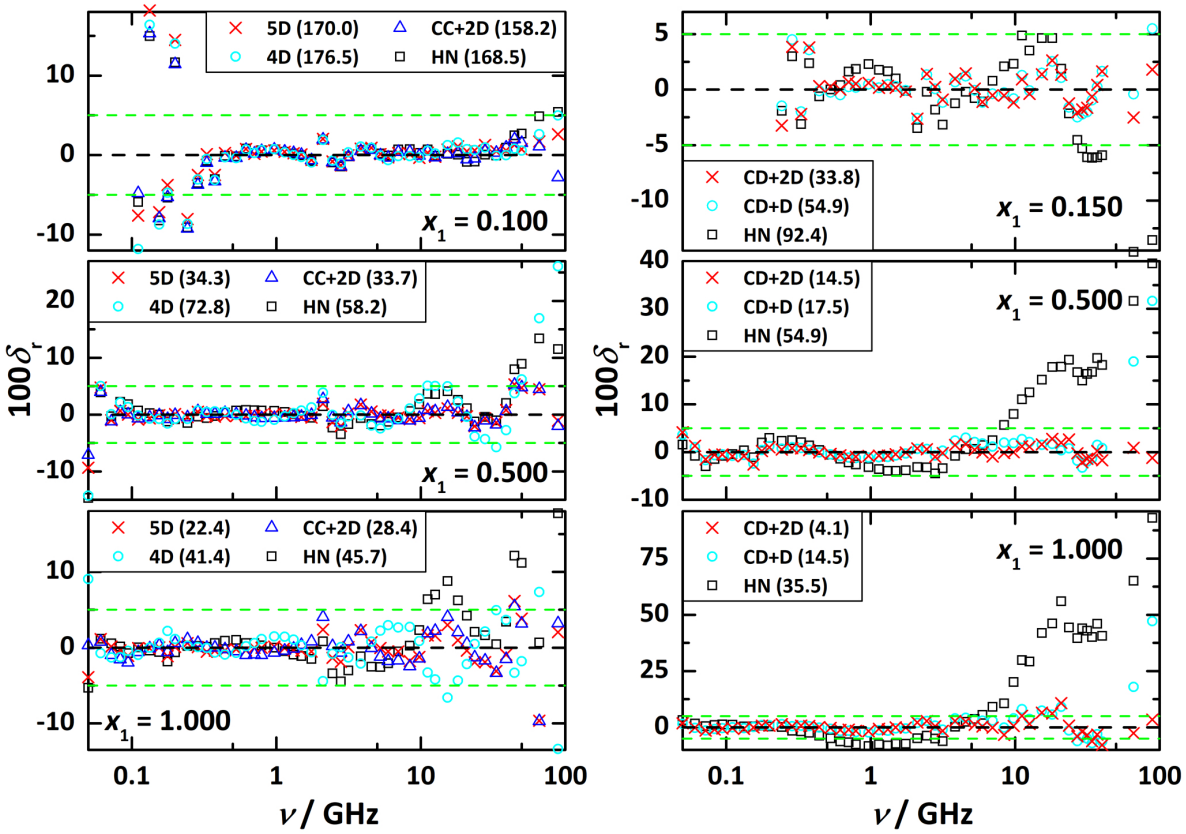

Figure S2: Relative deviations, δ_r, of the experimental dielectric loss, $\varepsilon''(\nu)$, from the corresponding fit values, $\varepsilon''_\mathrm{fit}(\nu)$, obtained with various models for glyceline/water (left panels) and reline/water (right panels) mixtures. For the first results for HN, CC+2D, 4D and 5D models are shown for DES mole fractions $x_1 = 0.100$ (top panel), 0.500 (middle) and 1.000 (bottom). For the second δ_r values for HN, CD+D and CD+2D are shown at $x_1 = 0.150$ (top), 0.500 (middle) and 1.000 (bottom). Black dashed lines indicate $\delta = 0$; green dashed lines represent arbitrary margins of $100\delta = 5$. Values $10^3 \times \chi^2_\mathrm{r}$ of the reduced error functions for the shown fits are given in parentheses in the insets. For clarity only every second experimental point is displayed.

Table S2: Glyceline mass fraction, w_1, and relaxation parameters (amplitudes, S_j, relaxation times, τ_j, static permittivity, ε_s, permittivity at infinite frequency, ε_∞) obtained with the 5D fit model for glyceline/water mixtures at $T = 298.15$ K and glyceline mole fraction, x_1.

x_1	w_1	S_1	S_2	S_3	S_4	S_5	τ_1/ps	τ_2/ps	τ_3/ps	τ_4/ps	τ_5/ps	ε_s	ε_∞
0.000	0.000	0.00	0.00	0.00	72.48	2.43	–	–	–	8.35	0.28	78.37	3.52
0.010	0.154	2.09	2.82	12.29	47.36	2.82	142	23.5	14.7	9.67	0.74	71.40	4.01
0.025	0.315	2.65	3.70	16.90	33.07	2.47	134	35.2	21.5	11.5	1.44	63.47	4.68
0.050	0.486	1.85	4.92	22.64	18.09	2.13	202	77.7	31.3	13.6	1.39	54.56	4.94
0.075	0.593	1.89	5.83	19.58	14.50	2.27	260	113	44.6	17.2	3.07	49.33	5.27
0.100	0.666	1.68	6.91	18.52	10.34	2.45	433	147	57.1	20.3	3.08	44.96	5.06
0.150	0.760	1.51	8.01	15.68	6.99	2.39	597	214	81.8	23.7	3.40	39.41	4.82
0.200	0.817	2.20	10.18	12.08	4.88	1.83	702	244	91.8	21.6	2.98	35.95	4.79
0.250	0.856	2.14	10.57	10.35	4.12	1.67	853	299	105	21.2	2.63	33.51	4.65
0.300	0.885	3.65	11.52	6.96	3.36	1.48	860	284	96.9	19.5	2.46	31.57	4.61
0.400	0.923	4.19	11.00	5.31	2.75	1.27	1100	339	102	18.7	2.32	29.05	4.54
0.499	0.947	5.13	10.39	4.25	2.40	1.12	1180	354	93.3	16.2	1.78	27.72	4.43
0.599	0.964	5.45	9.11	3.71	2.16	1.07	1110	373	94.7	16.3	1.94	25.91	4.41
0.699	0.976	6.87	7.72	3.00	1.98	0.95	989	332	82.6	14.8	1.77	24.96	4.43
0.800	0.986	6.17	7.55	3.09	1.92	0.87	1100	386	91.7	14.9	1.89	24.06	4.47
0.897	0.993	6.68	6.71	2.84	1.84	0.95	1070	370	86.4	13.7	1.28	23.26	4.25
1.000	1.000	6.53	6.44	2.78	1.78	0.89	1120	402	95.3	15.2	1.74	22.80	4.38

$\varepsilon''(\nu)$ values systematically deviate from the HN fit at $\nu > 10$ GHz, indicating additional high-frequency components. Whilst the 4D model performed worse than HN, significantly better fits were obtained with CC+2D and 5D at $x_1 \geq 0.100$. Both models yielded comparable χ^2_r values. However, in contrast to the 5D fit (Table S2; see main manuscript for the assignment of the resolved modes) the parameters of CC+2D did not extrapolate smoothly to the values of the 2D fit for neat water [7, 8] as for free-running optimization at $x_1 \leq 0.1$ the CC+2D model collapsed to CC+D. In this CC+D description the expelled fast water mode was compensated by broadening the CC mode. On the other hand, freezing the fast water relaxation time, τ_f, in the fit procedure at the level of $0.3 - 2.0$ ps (the results are shown in Fig. S3e-h) lead for CC+2D to breakpoints in the concentration dependencies of S_j & τ_j for $j = 2 - 3$ that could not be reasonably interpreted.

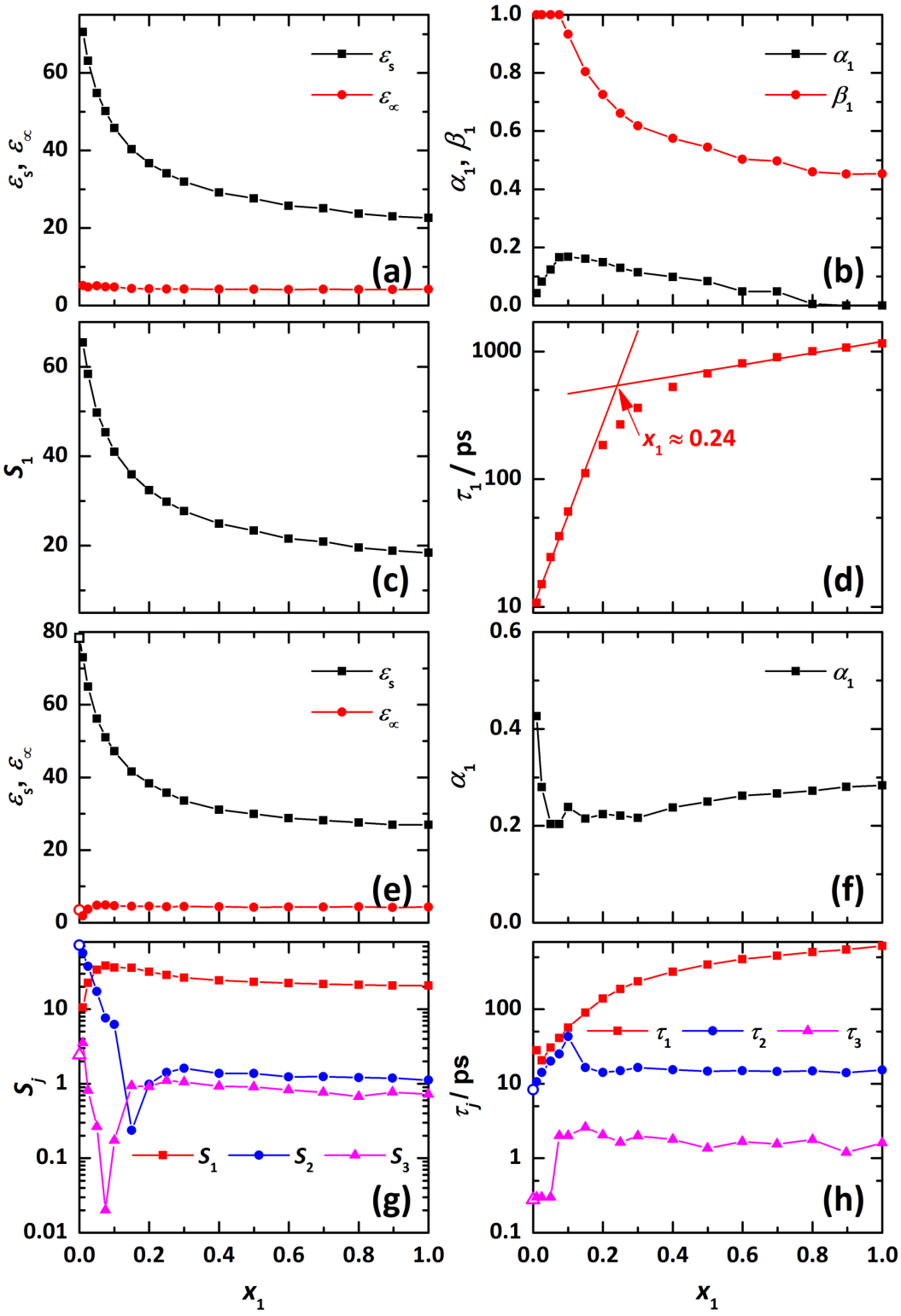

Figure S3: Selected fit parameters obtained with the HN (a-d) and CC+2D models (e-h) for glyceline/water mixtures: (a, e) static permittivity, ε_s, and high-frequency permittivity, ε_∞; (b, f) shape parameters α_1 and β_1 (b only); amplitudes, S_1 and S_2 (c, g), and associated relaxation times, τ_1 and τ_2 (d, h), as a function of DES mole fraction, x_1. Red solid lines in (c) represent linear fits of $\log \tau_1$ *vs.* x_1. Data for neat water [8] are indicated by open symbols.

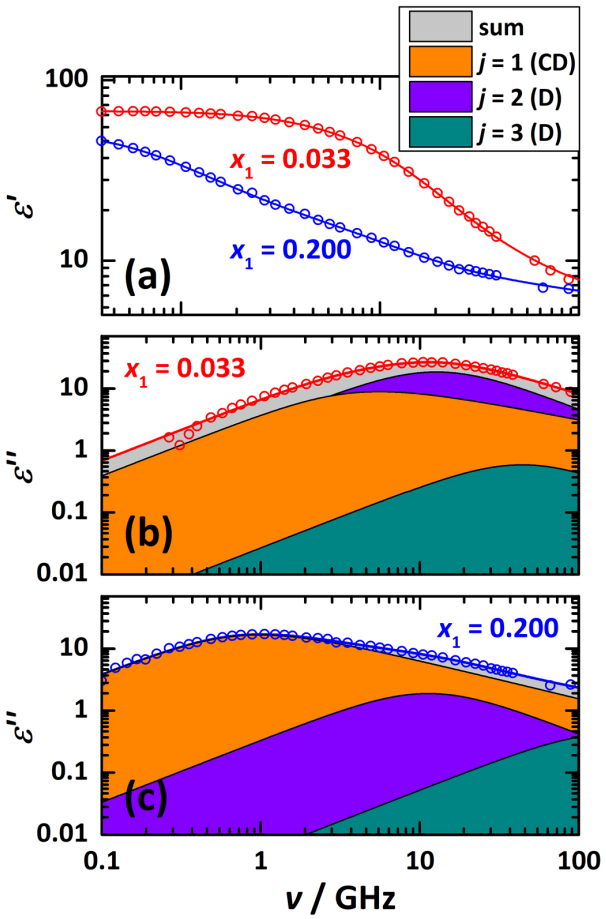

Figure S4: Spectra of relative permittivity, ε' (a), and dielectric loss, ε'' (b, c) of reline/water mixtures for $x_1 = 0.033$ (a & b) and $x_1 = 0.200$ (a & c). Symbols are experimental data, lines the result of the fit with the CD+2D model. The shaded areas in panels (b, c) show contributions of the resolved Cole-Davidson (CD; $j = 1$) and Debye (D; $j = 2,\ 3$) modes. For clarity only every second experimental point is shown.

Reline/water mixtures. The right panel of Fig. S2 compares relative deviations, δ_r, of $\varepsilon''(\nu)$ from the fit values, $\varepsilon''_{fit}(\nu)$, obtained for reline/water mixtures with the HN, CD+D and CD+2D models. Similar to glyceline/water, a single HN equation collapsing to CC fitted the experimental spectra well at $x_1 \leq 0.100$ but failed at higher DES contents with respect to χ^2_r and the desired smooth variation of fit parameters with x_1 (Fig. S5a-d).

The sudden change of the shape parameter from pure CC for $x_1 \leq 0.100$ to pure CD at $x_1 \geq 0.200$ suggested the rather abrupt emergence of higher-frequency components in the spectra. Consequently, the models HN+D, HN+2D, 4D and 5D were tested. It was found that the HN+2D model, where HN had collapsed to the CD equation (ie. the CD+2D model; $\alpha_1 = 0$) provided the best fit (Fig. S4, Table S3) with smooth variation of the obtained parameters. As discussed in detail in the main manuscript the two Debye modes at intermediate and high frequencies are readily assigned to water. In contrast to glyceline/water, where the Debye modes $j = 1$ and 3 could be assigned to hydrated glycerol and $j = 2$ to hydrated choline cation, it was not possible for reline/water to split the lower-frequency CD mode further although separate contributions from urea and Ch^+, thus a 4D model, could be anticipated. Possible reasons are discussed in the main manuscript.

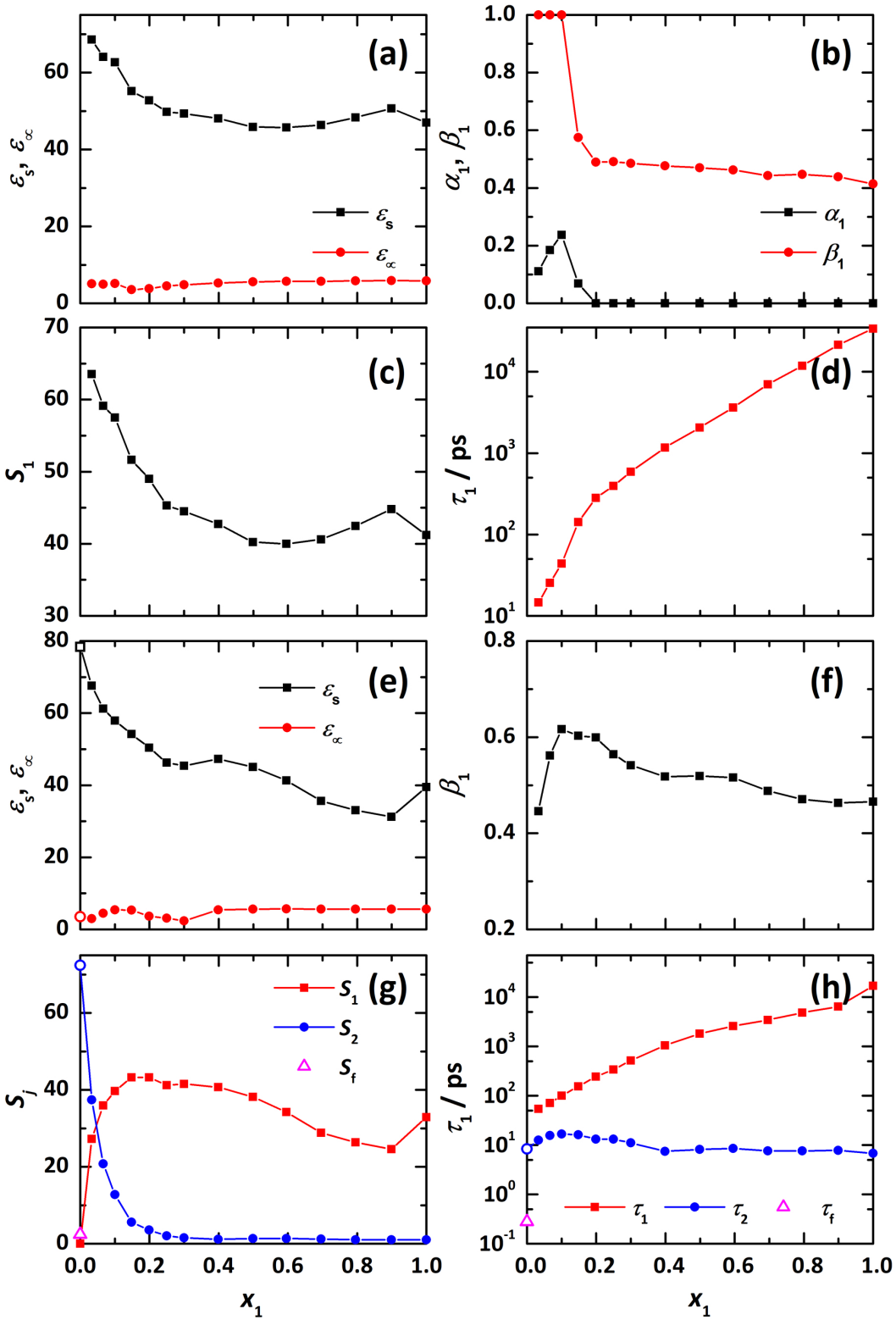

Figure S5: Selected fit parameters obtained with the HN (a-d) and CD+D models (e-h) for reline/water mixtures: (a, e) static permittivity, ε_s, and high-frequency permittivity, ε_∞; (b, f) shape parameters α_1 (b only) and β_1; (c, g) amplitudes, S_1 and S_2 (g only); (d, h) relaxation times, τ_1 and τ_2 (h only)), as a function of DES mole fraction, x_1. Data for neat water [8] are indicated by open symbols.

Table S3: Reline mass fraction, w_1, and relaxation parameters (amplitudes, S_j, relaxation times, τ_j, shape parameter of the Cole-Davidson mode, β_1, static permittivity, ε_s, permittivity at infinite frequency, ε_∞) at reline mole fraction, x_1, obtained with the CD+2D fit model for reline/water mixtures at $T = 298.15$ K and reline mole fraction, x_1.

x_1	w_1	S_1	S_2	S_3	τ_1	τ_2	τ_3	β_1	ε_s	ε_∞
0.000	0.000	0.00	72.48	2.43	0.00	8.35	0.28	–	78.37	3.52
0.033	0.329	25.22	37.13	1.18	49.4	12.5	3.62	0.50	67.38	3.85
0.067	0.507	35.35	20.93	0.93	68.9	15.2	0.15	0.59	61.17	3.97
0.100	0.615	39.20	12.19	1.01	91.2	15.9	0.38	0.64	57.08	4.68
0.148	0.715	39.95	7.43	1.03	143	16.5	1.78	0.68	53.93	5.52
0.199	0.782	40.24	4.53	1.38	229	18.0*	3.38	0.66	51.80	5.66
0.250	0.827	39.34	2.70	1.07	326	18.1	1.90	0.61	48.37	5.27
0.300	0.860	40.03	1.88	1.04	496	16.6	1.58	0.57	47.99	5.04
0.399	0.905	38.74	1.35	1.12	948	16.8	1.82	0.55	46.33	5.12
0.499	0.935	37.88	1.20	1.23	1770	12.6	0.88	0.53	45.05	4.73
0.596	0.955	37.69	1.09	1.05	3020	12.2	1.01	0.52	44.78	4.94
0.696	0.970	36.29	1.02	1.22	4850	11.4	0.83	0.51	43.25	4.72
0.796	0.982	35.99	1.00	1.50	7200	11.6	0.59	0.51	43.34	4.85
0.899	0.992	34.82	0.97	0.91	10300	11.3	0.89	0.50	41.71	5.02
1.000	1.000	34.44	0.85	0.92	16900	10.1	0.85	0.48	41.17	4.97

* Parameter fixed in fit procedure

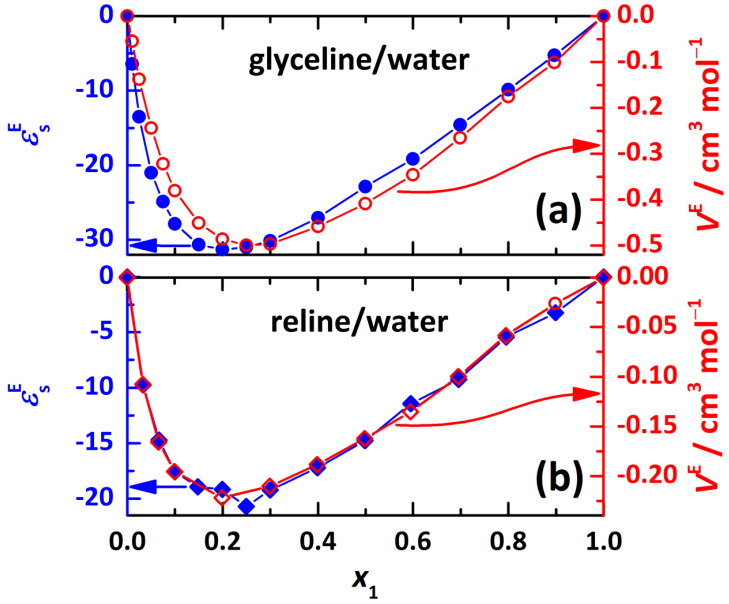

Figure S6: Excess molar permittivities, ε_s^E (solid symbols, left scale) and excess molar volumes, V^E (open symbols, right scale) obtained in glyceline/water (a) and reline/water (b) mixtures as a function of DES mole fraction, x_1. Arrows address the curves to appropriate axes.

S3 Effective dipole moments of possible dipolar species

Table S4: Effective dipole moments, μ_j^{eff}, of Ch^+, ChCl contact ion pairs (CIPs), urea and glycerol embedded in a continuous medium having the static permittivity of water ($\varepsilon_s = 78.36$), glyceline ($\varepsilon_s = 22.8$), or reline ($\varepsilon_s = 41.2$) as obtained with Gaussian at the 6-31++G(d,p) level of theory [10]. Also included are the associated cavity field factors, A_j, of the dipoles calculated from the Gaussian output.

species	μ_j^{eff}(in water)/D	μ_j^{eff}(in glyceline)/D	μ_j^{eff}(in reline)/D	A_j
Ch^+	4.56	4.49	4.52	0.216
CIP	17.69	17.27	17.53	0.313
urea	5.93	–	5.91	0.300
glycerol	4.23	4.21	–	0.321

References

[1] V. Agieienko and R. Buchner, *J. Chem. Eng. Data*, 2019, **64**, 4763–4774.

[2] T. P. Marsland and S. Evans, *IEE Proc., Part H*, 1987, **134**, 341–349.

[3] S. Schrödle, G. Hefter, W. Kunz and R. Buchner, *Langmuir*, 2006, **22**, 924–932.

[4] J. Barthel, K. Bachhuber, R. Buchner, H. Hetzenauer and M. Kleebauer, *Ber. Bunsenges. Phys. Chem.*, 1991, **95**, 853–859.

[5] A. Stoppa, A. Nazet, R. Buchner, A. Thoman and M. Walther, *J. Mol. Liq.*, 2015, **212**, 963–968.

[6] P. R. Bevington and D. K. Robinson, *Data Reduction and Error Analysis for the Physical Sciences*, McGraw-Hill, New York, 3rd edn., 2003.

[7] T. Fukasawa, T. Sato, J. Watanabe, Y. Hama, W. Kunz and R. Buchner, *Phys. Rev. Lett.*, 2005, **95**, 197802.

[8] A. Eiberweiser, A. Nazet, G. Hefter and R. Buchner, *J. Phys. Chem. B*, 2015, **119**, 5270–5281.

[9] F. Kremer and A. Schönhals, *Broadband Dielectric Spectroscopy*, Springer, Berlin, 2003.

[10] M. J. Frisch, G. W. Trucks, H. B. Schlegel, G. E. Scuseria, M. A. Robb, J. R. Cheeseman, G. Scalmani, V. Barone, B. Mennucci, G. A. Petersson, H. Nakatsuji, M. Caricato, X. Li, H. P. Hratchian, A. F. Izmaylov, J. Bloino, G. Zheng, J. L. Sonnenberg, M. Hada, M. Ehara, K. Toyota, R. Fukuda, J. Hasegawa, M. Ishida, T. Nakajima, Y. Honda, O. Kitao, H. Nakai, T. Vreven, J. Montgomery, J. A., J. E. Peralta, F. Ogliaro, M. Bearpark, J. J. Heyd, E. Brothers, K. N. Kudin, V. N. Staroverov, R. Kobayashi, J. Normand, K. Raghavachari, A. Rendell, J. C. Burant, S. S. Iyengar, J. Tomasi, M. Cossi, N. Rega, J. M. Millam, M. Kiene, J. E. Knox, J. B. Cross, V. Bakken, C. Adamo, J. Jaramillo, R. Gomperts, R. E. Stratmann, O. Yazyev, A. J. Austin, R. Cammi, C. Pomelli, J. W. Ochterski, R. L. Martin, K. Morokuma, V. G. Zakrzewski, G. A. Voth, P. Salvador, J. J. Dannenberg,

S. Dapprich, A. D. Daniels, O. Farkas, J. B. Foresman, J. V. Ortiz, J. Cioslowski and D. J. Fox, *Gaussian 09, Revision B.01*, Gaussian Inc.: Wallingford CT, 2010.